EARTHQUAKE SAFTEY ASSESSMENT OF A TALL BRICK CHIMNEY IN TOKONAME BASED ON THE MICRO-TREMOR MEASUREMENT

T. Yamamoto[1] and T. Maeda[2]

[1] *Graduate Student, Dept. of Architecture, Waseda University, Tokyo. Japan*
[2] *Professor, Dept. of Architecture, Waseda University, Tokyo, Japan*
Email: takeya0713@akane.waseda.jp

ABSTRACT :

This paper deals with earthquake safety of the brick chimney of the height of 23 m in Tokoname, Japan. We measured micro-tremor to acquire vibration characteristics, which was used to construct FE model for the superstructure by simulating base-fixed horizontal natural frequencies. Soil-foundation interaction was treated by installing soil springs which were determined by simulating soil-coupled frequency. With the soil-coupled FE model, linear dynamic response analysis was carried out for four kinds of input ground motions. It is found that the base of the chimney will have damage at maximum acceleration from 41 to 77 Gal, should the collapse be caused by excessive tensile stress at mortal joints.

KEYWORDS: brick chimney, micro-tremor, Tokoname, soil spring, soil-structure interaction

1. Introduction

Tokoname is a well-known pottery town in Chita Peninsula, Aichi Prefecture, Japan. Many brick chimneys for pottery works were built from the end of 19th century to the middle of 20th century. Nowadays, more than half of them are not used for their original purpose; however, they are typical of the scenery in Tokoname to be preserved as a symbol of the town. Since Japan is an earthquake prone country and Tokoname is located in the anticipated damage area for the expected Tokai Earthquake in the Suruga Bay, these brick chimneys must be prepared for severe earthquake ground motion. We had an opportunity to study about earthquake safety of one of the tallest chimneys (Fig.1) which was built in 1922. The chimney is 23 m high and covers the area of 2.34 m square. The elevation and the section of the chimney are shown in Fig.2. Since the design drawings were not available, the section was estimated by referring to the drawings of similar chimneys and interviewing chimney craftsmen.

First of all, we measured micro-tremor to acquire vibration characteristics of the chimney and construct a FE model for its superstructure by simulating base-fixed natural frequencies. From measurements we found that rocking motion was predominant, which means soil-foundation interaction should be properly incorporated in dynamic response analysis as shown in the case of a HP type RC shell tower (Maeda *et al.* 2004). The importance of soil-foundation interaction for a tall brick chimney was also pointed out in the reference (Aoki *et al.* 2005). In the study about a masonry belltower (Ivorra *et al.* 2004), this effect was considered by the 3D soil model. In our study, it was treated by soil springs at the foundation for simplicity. The soil springs were determined by simulating soil-coupled frequencies by the soil-coupled FE model composed of superstructure model, the foundation, and the soil springs. With the soil-coupled FE model, the responses of the chimney to several major earthquake ground motions were computed to evaluate safety of the chimney against severe earthquake ground motion.

2. Micro-tremor Measurements

2.1. Measurement Cases

Six measurement cases for micro-tremor are shown in Tab.1. The case TB is for fundamental vibration characteristics in X and Y directions; the cases of RX and RZ are for the effects of rocking motion, the cases XX, XY, and YX are for mode shapes in X and Y directions. The coordinates used for measurements are shown in Fig.3. The sensor ID is composed of height defined in Fig.3, face ID, and measuring component. For example, face ID X_P means the face intersected by X axis at X positive and X_M at X negative. We will drop P and M, if we do not have to identify the face location explicitly.

Over-damped sensors for accelerations, GPL with three components and JEP's with one component were used for the case TB; acceleration data was filtered at 30 Hz and sampled by 1/100 second. Servo-type sensors for accelerations, LS-10C's, were used in other cases; acceleration data was filtered at 100 Hz and sampled by 1/256 second. Duration of measurements was 20 minutes for all the cases.

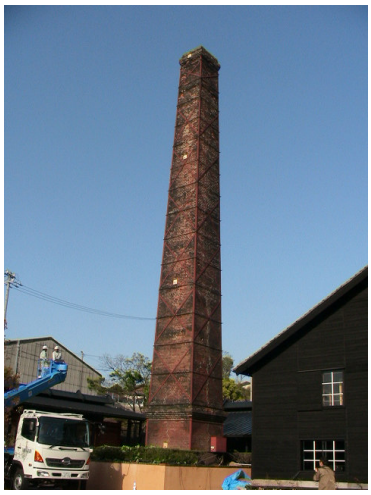

Figure 1 Appearance of the chimney

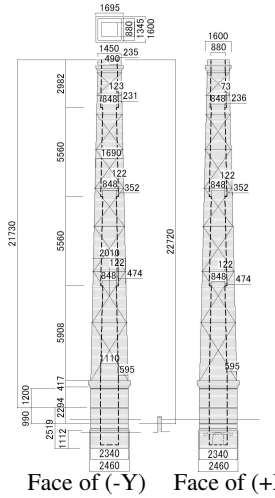

Figure 2 Elevation (solid line) and section (dot line)

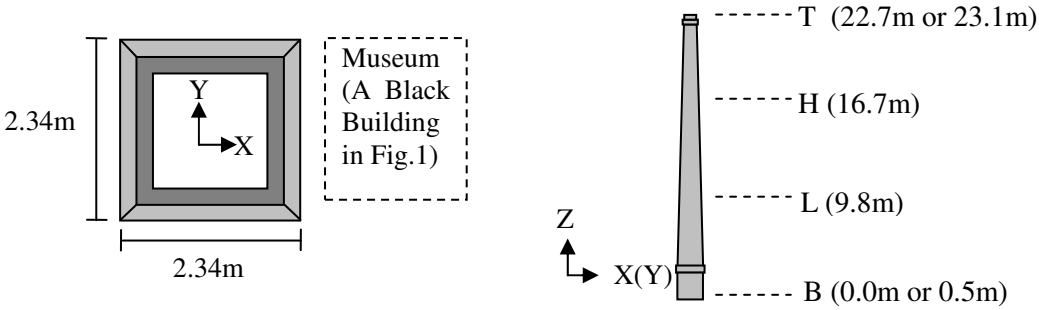

Figure 3 Definition of the coordinates

Table 1 Measurement cases and sensor arrangements

Case	ID	Face	Height	Component	Sensor
TB	TYY	−Y	23.1m	+Y	JEP
	TXX	−X	23.1m	+X	
	TXY	−X	23.1m	+Y	
	BXZ	X	0.0m	+Z	GPL
	BXY	X	0.0m	+Y	
	BXX	X	0.0m	+X	
RX	TXX	−X	22.7m	−X	LS−10C
	BX_MZ	−X	0.5m	+Z	
	BXX	−X	0.5m	−X	
	BX_PZ	X	0.5m	+Z	
RZ	TXZ	−X	22.7m	+Z	LS−10C
	BX_MZ	−X	0.5m	+Z	
	BXX	−X	0.5m	−X	
	BX_PZ	X	0.5m	+Z	

Case	ID	Face	Height	Component	Sensor
XX	BXX	−X	0.5m	−X	LS−10C
	LXX	−X	9.8m	−X	
	HXX	−X	16.7m	−X	
	TXX	−X	22.7m	−X	
XY	BXY	−X	0.5m	+Y	LS−10C
	LXY	−X	9.8m	+Y	
	HXY	−X	16.7m	+Y	
	TXY	−X	22.7m	+Y	
YX	BYX	−Y	0.5m	−X	LS−10C
	LYX	−Y	10.1m	−X	
	HYX	−Y	16.7m	−X	
	TYX	−Y	22.7m	−X	

2.2. Results of Measurements

Time history of TXX of the case TB shown in Fig.4. depicts poor stationary characteristics, which is common for other data and may be attributable to strong gusty wind during measurements. Power spectra of TXX, HXX, LXX and BXX of the case XX indicate clear peaks around 1 Hz, 4 Hz, and 9 Hz as shown in Fig.5. A power spectrum of TXZ of the case RZ also shows these clear peaks in Fig.6. Band-pass filtered time history of the case XX, shown in Fig.7, depicts in-phase motion around 1 Hz with increasing amplitude with height, which is considered as the 1st horizontal mode in X direction. Similarly, higher horizontal modes are identified at 4.2 Hz, 9.4 Hz, and 15.9 Hz. The 1st vertical mode is inferred at 10.8 Hz. Fig.8 shows power spectra of BXX, BX_PZ and BX_MZ of the case RX, and Fig.9 shows power spectrum of rocking angle θ, which is defined by Eqn.1, where w stands for the bottom width of the chimney. These figures represent that sway and rocking motion predominate around 1 Hz.

$$\theta = (BX_PZ - BX_MZ) / w \quad (1)$$

A spectrum ratio of TXX to the sum of the sway BXX and top rocking motion hθ of the case RX is shown in Fig.10, where h stands for the height of the chimney. This spectrum ratio may correspond to the base-fixed transfer function. In Fig. 10, the 1st natural frequency can not be identified, which is possibly due to the multi-input effects of wind and ground motion. A spectrum ratio of TXZ to the average of BX_PZ and BX_MZ is shown in Fig.11, which

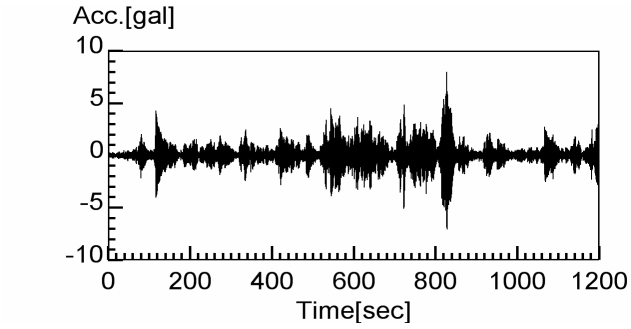

Figure 4 Acceleration time history of TXX

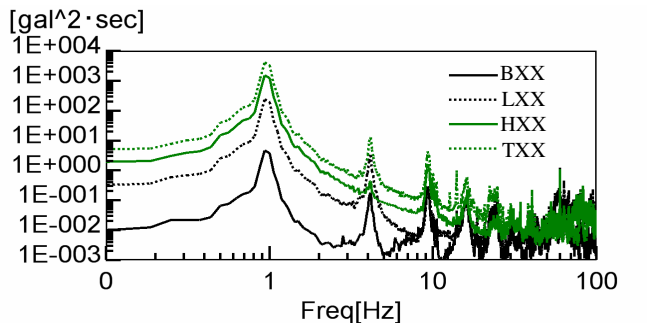

Figure 5 Power spectra of TXX, HXX, LXX and BXX

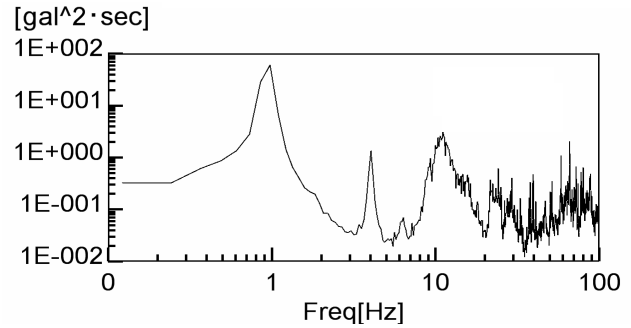

Figure 6 Power spectrum of TXZ

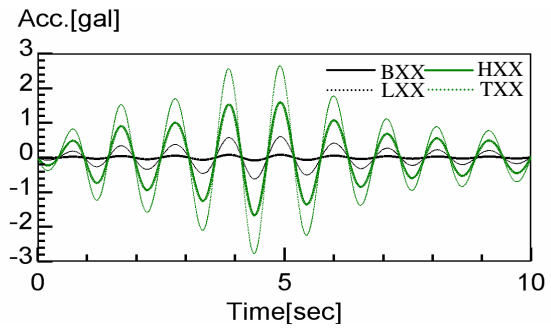

Figure 7 Band-pass filtered time history of TXX

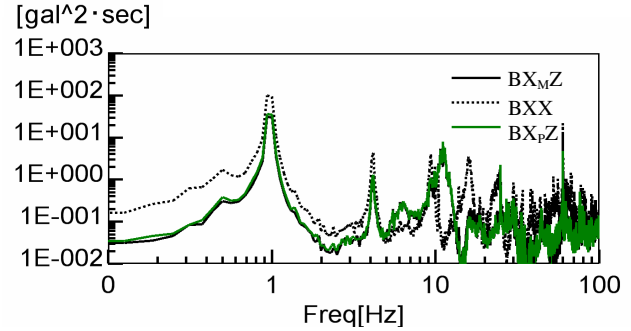

Figure 8 Power spectra of BXX, BX_PZ and BX_MZ

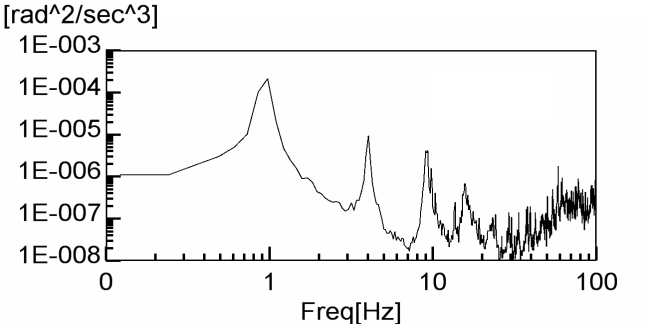

Figure 9 Power spectrum of rocking angle θ

corresponds to the base-fixed transfer function of vertical translation. From these figures, base-fixed natural frequencies for the 2nd and higher horizontal modes in X direction are evaluated at 5.9 Hz, 12.4 Hz, 21.8 Hz, and for 1st vertical mode at 13.9 Hz as summarized in Tab.2. Spectrum ratio of the sway BXX, top rocking motion hθ, and elastic deformation to TXX are shown in Fig.12, which represents sway ratio 0.03, rocking ratio 0.36 and elastic deformation ratio 0.60 in X direction around 1Hz.

Table 2 Predominant frequencies

	X direction				Z direction
	1st	2nd	3rd	4th	1st
Soil-coupled	1.0	4.2	9.4	15.9	10.8
Base-fixed	–	5.9	12.4	21.8	13.9

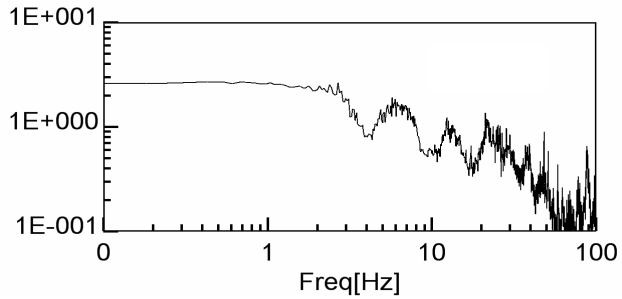

Figure 10 Spectrum ratio of TXX to the sum of BXX and hθ

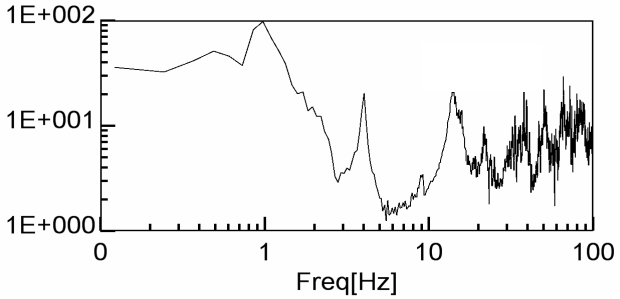

Figure 11 Spectrum ratio of TXZ to the average of BX_PZ and BX_MZ

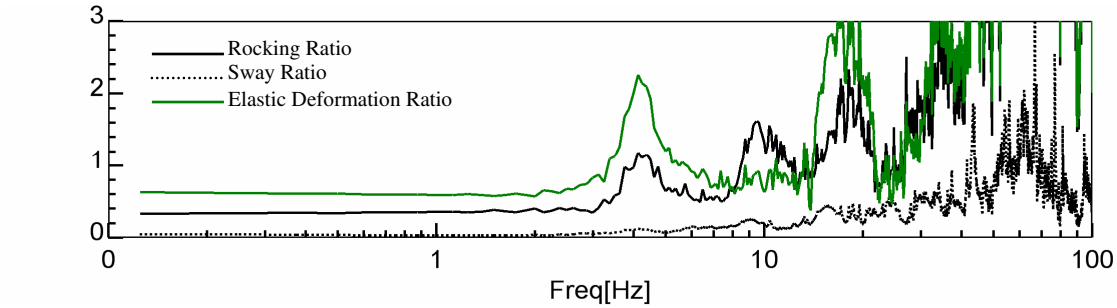

Figure 12 Spectrum ratios of sway, top rocking motion and elastic deformation to TXX obtained by measurement

3. FEM Modeling

3.1. Superstructure Model

The 3D FE model for the superstructure was constructed by 8-nodes solid elements, referring to Fig.2. The properties of a brick are specified referring to the literature (Aoki *et al.* 2005), e.g., mass density 1.65 g/mm^3, Poisson's ratio 0.2. Young's modulus of the brick was estimated as 2,730 N/mm^2 by equating the 2nd base-fixed natural frequency obtained by eigen-value analysis to that evaluated by micro-tremor measurement, which is not far from the material test data of bricks around Tokoname. Comparison of base-fixed natural frequencies at higher modes is summarized in Tab.3. Horizontal modes of the FE model are shown in Fig.13.

Table 3 Base-fixed predominant frequencies by measurement and analysis

	X direction				Z direction
	1st	2nd	3rd	4th	1st
Measurement (base-fixed)	–	5.9	12.4	21.8	13.9
Analysis (base-fixed)	1.4	5.9	13.8	24.1	18.1

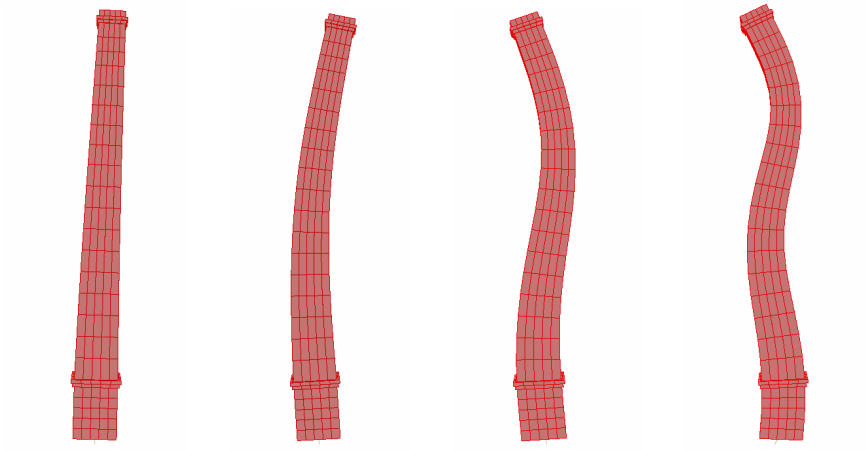

Figure 13 Horizontal translation modes of the FE model

3.2. Soil Springs

The effects of soil-structure interaction were incorporated by soil springs attached to the superstructure FE model. By simulating the 1st horizontal soil coupled predominant frequency of 1.0 Hz, soil springs were estimated as Kv=7.1×10^5 kN/m for vertical, Kh=5.3×10^5 kN/m for horizontal, and Kr=9.1×10^5 kN･m/rad for rocking. Assuming mass density of soil 1.6g/mm^3 and Poisson's ratio 0.4, equivalent shear wave velocity for the half-space is 220m/s and associated damping coefficients at 1.0Hz are Cv=1.0×10^4 kN･s/m for vertical, Ch=5.4×10^3 kN･s/m for horizontal, and Cr=1.1×10^2 kN･m･s/rad for rocking from the reference (Architectural Institute of Japan 1996).

3.3. Vibration Characteristics

Fig.14 shows computed power spectrum of horizontal motion at the top due to white noise input with 1 % of material damping for solid elements. Predominant frequencies compare well with soil-coupled predominant frequencies evaluated by measurements as summarized in Tab.4. Spectrum ratios of sway, top rocking motion and elastic deformation to TXX are shown in Fig.15; the value around 1Hz are summarized in Tab.5. Despite the fact that the 1st base-fixed natural frequency was not adequately obtained, the 1st mode should be contributing most to the earthquake ground motion; thus we simulated the 1st soil-coupled frequency by soil springs.

Table 4 Soil-coupled predominant frequencies for X direction by measurement and analysis

	1st	2nd	3rd	4th
Measurement (soil-coupled)	1.0	4.2	9.4	15.9
Analysis (soil-coupled)	1.0	4.7	11.6	19.3

Table 5 Sway ratio, rocking ratio and elastic deformation ratio at 1.0Hz by measurement and analysis

	Sway Ratio	Rocking Ratio	Elastic Deformation Ratio
Measurement (soil-coupled)	0.03	0.36	0.60
Analysis (soil-coupled)	0.02	0.48	0.50

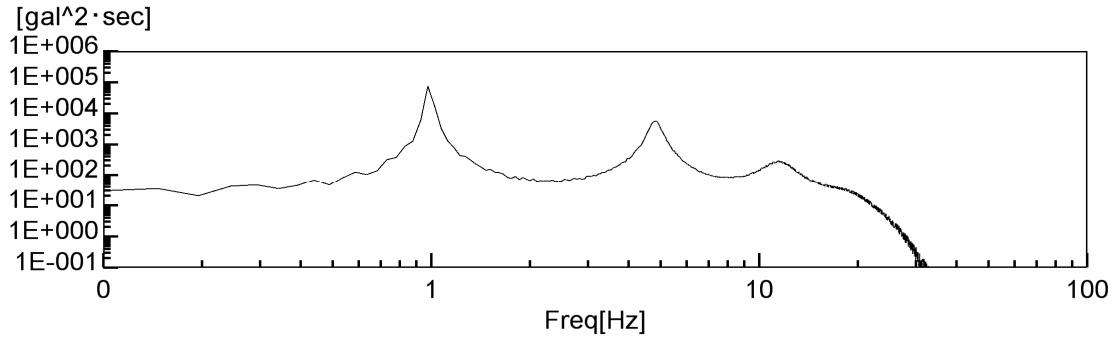

Figure 14 Power spectrum of TXX

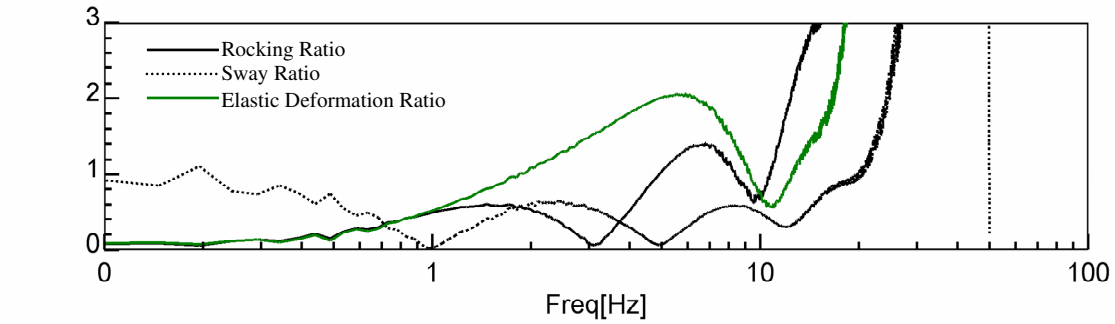

Figure 15 Spectrum ratios of sway, top rocking motion and elastic deformation to TXX obtained by analysis

4. Response Analysis to Earthquake Ground Motion

4.1. Seismic Response Analyses

Linear dynamic response analysis was carried out with the soil-coupled FE model. Input earthquake ground motion were El Centro 1940 NS, Taft 1952 EW, Hachinohe 1968 NS, JMA Kobe 1995 NS; all of them were normalized to PGV of 25 kine, which is regarded as rare ground motion of level 1 in Japan for high-rise buildings to behave elastically. Acceleration response spectra of these ground motion are shown in Fig. 16. Maximum response of absolute acceleration and relative velocity are 1,422 Gal and 180 kine at the top of the chimney for El Centro 1940. Maximum relative displacement is 282 mm for Hachinohe 1968. Maximum base shear coefficient is 0.26 for Taft 1952. Maximum response parameters are shown in Tab.6. Distributions of absolute acceleration, relative velocity, relative displacement, shear force and overturning moment with height are shown in Fig.17 to Fig.21; common legend is represented in Fig. 17. Maximum tensile stresses are occurred in the same base element in Fig.22, irrespective of ground motions. Fig.23 shows acceleration response spectra at the top, where the 1st mode is predominant.

Table 6 Summary of seismic response analyses

	PGA [Gal]	Max. Absolute Acceleration [Gal]	Max. Relative Velocity [kine]	Max. Relative Displacement [mm]	Max. Base Shear Coef. [shear force/total weight]
El Centro NS	245	1422	180	260	0.25
Taft EW	250	1229	146	218	0.26
Hachinohe NS	167	1204	175	282	0.18
JMA Kobe NS	220	1096	167	263	0.22

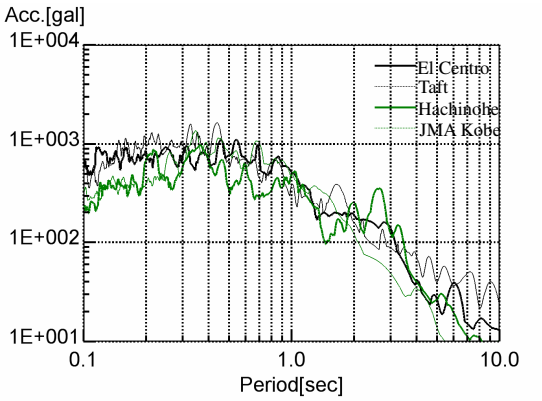

Figure 16 Acceleration response spectra of ground motion (h = 1%)

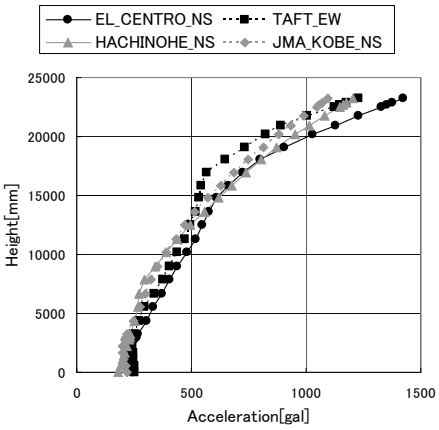

Figure 17 Maximum response acceleration

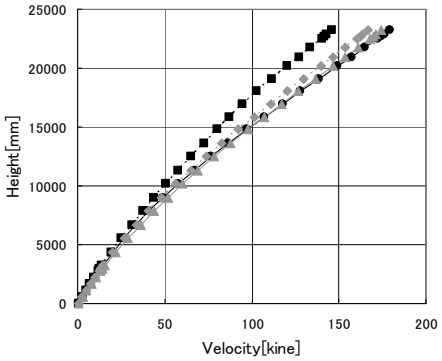

Figure 18 Maximum response velocity

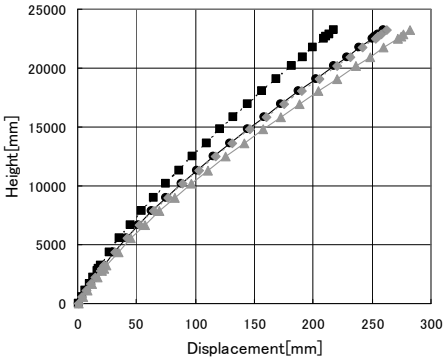

Figure 19 Maximum response displacement

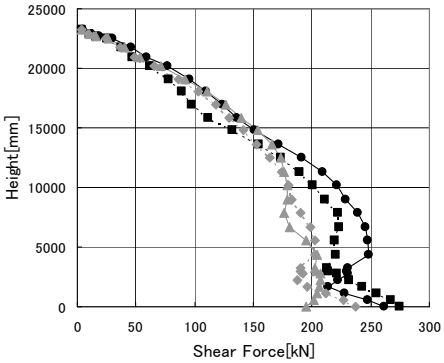

Figure 20 Maximum shear force

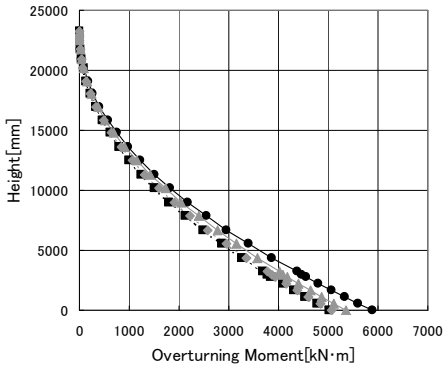

Figure 21 Maximum overturning moment

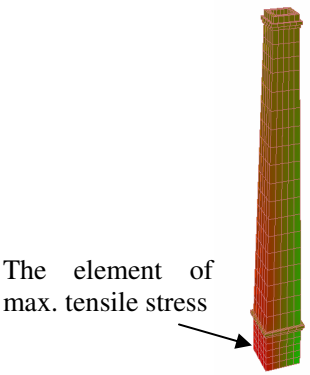

Figure 22 Distribution of normal stress σ_t

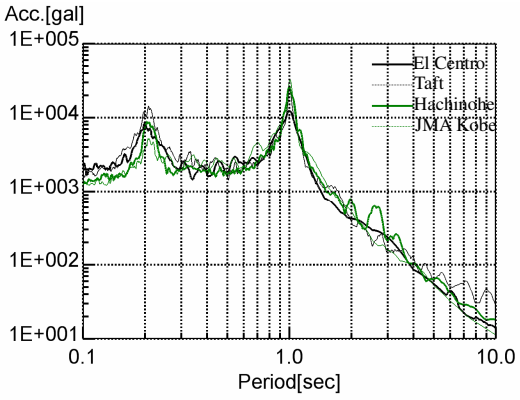

Figure 23 Acceleration response spectra at the top (h = 1%)

4.2. Consideration of Seismic Safety

Collapse of the chimney may be started at the base due to excessive tensile stress at mortal joints. If we assume tensile strength of mortal as $f_t = 0.37$ N/mm^2 following the literature (Aoki *et al.* 2005), and compression stress due to gravity taken into account, maximum acceleration limit will be from 41 to 77 Gal, as shown in Tab.7. These accelerations are less than 1/3 of that of input ground motion of maximum velocity of 25 kine revealing inadequate seismic safety to the anticipated Tokai Earthquake.

Table 7 Maximum tensile stress and estimated PGA limit

	PGA [Gal]	σ_t Max. Tensile Stress [N/mm^2]	σ_c Stress by Gravity [N/mm^2]	$(\sigma_t + \sigma_c) / f_t$	PGA Limit [Gal]
El Centro NS	245	2.369	−0.268	5.68	66
Taft EW	250	2.081	−0.268	4.90	77
Hachinohe NS	167	2.615	−0.268	6.34	41
JMA Kobe NS	220	2.421	−0.268	5.82	58

5.Conclusions

A tall brick chimney in Tokoname was inspected against strong earthquake ground motion. By micro-tremor measurements, vibration characteristics were obtained and predominated rocking motion was recognized. The 3D FE model for the superstructure was constructed and Young's modulus of the brick was estimated as 2,730 N/mm^2 by simulating the 2nd horizontal base-fixed predominant frequency. The effect of soil-structure interaction was taken into account by soil springs. With the soil-coupled FE model, linear dynamic response analysis was carried out for four types of earthquake ground motion. If the collapse of the chimney is caused by excessive tensile stress at mortal joints, maximum acceleration limit will be from 41 to 77 Gal and the chimney will be toppled at the base. These accelerations are less than 1/3 of that of input ground motion normalized to maximum velocity of 25 kine, revealing inadequate seismic safety to the anticipated Tokai Earthquake ground motion.

REFERENCES

Aoki, T. and Sabia, D. (2005). Structural identification and seismic performance of brick chimneys, Tokoname, Japan, *Structural Engineering and Mechanics* **21:5,** 553-570.

Architectural Institute of Japan (1996). An Introduction to Dynamic Soil-Structure Interaction, Maruzen, Tokyo, Japan (in Japanese).

Ivorra, S., Pallarés, F., and Adam, J.M. (2008). Experimental and numerical studies on the belltower of Santa Justa y Rufina (Orihuela-Spain), *Proceedings of the sixth international conference on Structural Analysis of Historic Construction***,** 349-355.

Maeda, T., Kurauchi, N., and Sugiura, Y. (2004). Vibration characteristics of a HP type RC shell water tower acquired by micro tremor observation, *AIJ Journal of Technology and Design* **19,** 101-104 (in Japanese).